Hydrothermal Liquefaction of *Salix psammophila* in the Presence of Ionic Liquid and Water

Chun Li,[a] Youwen Wang,[a] Yongsheng Bian,[b] Jianguo Ren,[c] Jingjing Zhang,[a] Yunong Tang,[a] Xiaolin Yan,[a,*] and Xiaotao Zhang [a,*]

Salix psammophila was converted to value-added chemicals in the presence of 1-butyl-3-methylimidazolium chloride ([Bmim]Cl) and water by the hydrothermal liquefaction method. [Bmim]Cl acted as both liquefier and catalyst, while water served as both co-solvent and reactant. The optimal reaction parameters for the highest liquefaction yield were determined by an orthogonal experiment. The possibility of application of the recycled [Bmim]Cl was investigated. FT-IR spectra results of the fresh used, the firstly reused, and the secondary reused IL [Bmim]Cl confirmed the high stability of [Bmim]Cl. Moreover, an explanation of the possible liquefaction mechanism for *S. psammophila* was also provided. This study may provide fundamental data for *S. psammophila* conversion and application.

DOI: 10.15376/biores.18.4.7341-7352

Keywords: Salix psammophila; [Bmim]Cl; Hydrothermal liquefaction; Orthogonal experiment; Recyclability

*Contact information: a: College of Science, Inner Mongolia Agriculture University, Hohhot 010018, China; b: CHN Energy Yulin Chemical Co., Ltd., Yulin, China; c: Inner Mongolia Donghua Energy Co., Ltd., Ordos, China; *Corresponding authors: 13947113956@163.com; lianzixiaotao@163.com*

INTRODUCTION

The desert shrub *Salix psammophila* is one of the typical sand-fixing plants in northwestern China. It is a natural, abundant, and renewable biomass feedstock. It is planted to fix wind-blown sand on the ground surface and control desertification. However, it is necessary to cut the parts of *S. psammophila* above ground every 3 to 5 years to allow it to regenerate and maintain a sustainable ecological system, producing a large amount of *S. psammophila* branch residues (Ji *et al.* 2019). Harvested *S. psammophila* has traditionally been used as a fuel, animal fodder, raw materials of boards and pulp, and herbal medicines, *etc.* (Kubo *et al.* 2013). Recently, researchers have found that the potential of liquefied *S. psammophila* can be exploited as chemicals (Li *et al.* 2013). Therefore, the full exploitation of *S. psammophila* plants for high-value alternative fuels and chemicals is meaningful and feasible.

As a lignocellulosic biomass, cellulose, hemicellulose, and lignin are the main components of *S. psammophila*. In recent years, the liquefaction of this plant under sulfuric acid, nitric acid, or hydrochloric acid catalysis have been studied (Zhong *et al.* 2020, 2022). However, it is well established that the highly hydrogen-bonded cellulose component cannot be easily dissolved in any conventional solvents (Maldas and Shiraishi 1997).

Ionic liquids (ILs) are environmentally friendly molten salts with advantages of high polarities, low melting point, non-volatility, and they are identified as promising green solvents for lignocellulosic biomass dissolution (Yoo *et al.* 2017). The solubility of

cellulose varies to an extreme extent with the chosen IL, because it depends on the ability of IL to disrupt the inter-chain hydrogen bonds in cellulose (Schenzel *et al.* 2014). Among various ILs, 1-butyl-3-methylimidazolium chloride ([Bmim]Cl) has been first studied for cellulose dissolution by Swatloski *et al.* (2002). Numbers of reports about [Bmim]Cl have been published for cellulose pretreatment and utilization (Vitz *et al.* 2009; Schenzel *et al.* 2014; Reina *et al.* 2016) since then, but few have discussed *S. psammophila* liquefaction.

The hydrothermal liquefaction process is a transformation process that involves very complex reactions and takes place at very high temperatures (220 to 380 °C) and pressures (5 to 25 MPa) in the water solvent environment with and without catalyst (Durak *et al.* 2019, 2023). Though hydrothermal liquefaction of biomass to obtain bio-based chemicals has been investigated extensively (Gollakota *et al.* 2018), reports on hydrothermal liquefaction of *S. psammophila* with IL [Bmim]Cl are scare.

Herein, hydrothermal liquefaction of *S. psammophila* in the presence of ([Bmim]Cl) and water were studied. The effects of temperature, reaction time, and solid-liquid ratio (mass ratio of *S. psammophila* to ([Bmim]Cl)) on liquefaction process were investigated. Liquefied products were examined by using GC analysis. Recyclability of ([Bmim]Cl) were also tested.

EXPERIMENTAL

Materials and Reagent

Salix psammophila plants were harvested from Ordos, Inner Mongolia, China. Samples used in the liquefaction were dried at 105 °C for 24 h, grounded, and sieved through a 40-mesh sieve. 1-Butyl-3-methylimidazolium chloride ([Bmim]Cl) was purchased from Aolike Chemical Reagents Co., Ltd., Lanzhou, China. Ethyl acetate and ethanol used were of analytical grade obtained from Guangfu Reagents Co., Ltd. (Tianjin, China).

Liquefaction reaction and product separation procedure

[Bmim]Cl and *S. psammophila* with various solid-liquid ratios (1:0.5, 1:1, 1:1.5) were charged into a reaction kettle (100 mL, WHF-0.1, Weihai control the reaction kettle Co., Ltd.), and mixed with 50.0 mL distilled water. The reaction kettle was set at varying temperatures (180, 200, and 240 °C). When the temperature reached the set value, it was maintained for the definite reaction time (30, 60, or 150 min). After the desired reaction time, the reaction kettle was cooled to room temperature and the total reaction products in the autoclave were fully collected.

The separation procedure of the reaction products is illustrated in Fig. 1. As shown, the collected brown reaction products were first washed by 25.0 mL ethyl acetate, then the solid phase and filtrate were obtained after centrifugation. 25.0 mL ethanol was used to wash the solid phase and to remove the [Bmim]Cl, the final solid residue was dried at 105 °C to a constant weight. The liquefaction ratio (%) of the *S. psammophila* was calculated by the following equation:

$$\text{Liquefaction ratio (\%)} = \left(1 - \frac{\text{mass of residue}}{\text{mass of } S.psammophila}\right) \times 100\% \quad (1)$$

The filtrate was separated using a separatory funnel. The obtained supernatant was used for gas chromatography (GC) analysis as oil phase products with ethyl acetate and the

water phase with [Bmim]Cl was separated. The aqueous solution was then evaporated in a rotary evaporator to recycle [Bmim]Cl.

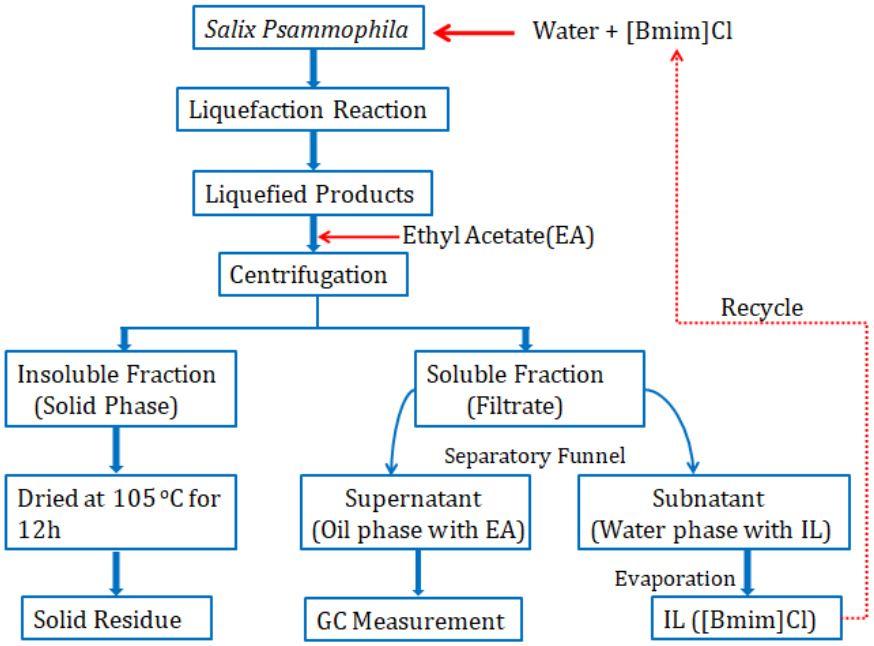

Fig. 1. The procedure for liquefied products separation

The analysis of liquefied products

The liquefied products were verified using GC (Agilent 7820A, Santa Clara, CA, USA) equipped with a DB-1 column by external standard method. The injector temperature was set at 230 °C, and the injection volume was 1.0 μL. The working conditions were set as follows: the column temperature increased to 40 °C and held for 2 min, then ramped to 200 °C at a heating rate of 10 °C·min^{-1} and held for 3 min. Subsequently, the column temperature decreased to 40 °C at a heating rate of 30 °C·min^{-1}; the whole running time was 25 min. The chromatograph used a split/splitless injector and a flame ionization detector (FID) with a 1:10 hydrogen (30 mL·min^{-1})/air mixture (300 mL·min^{-1}) as the flame fuel. The carrier gas used was dry, high-purity nitrogen. The detector temperature was adjusted to 260 °C.

Range analysis

In a range analysis, there are two parameters, K_i and R. K_i is defined as the sum of the indexes of the same level in each factor. The quantity k_i is the average value of K_i. A higher value k_i demonstrates that the corresponding level has a bigger effect; R is defined as the range between the maximum and minimum value of k_i. R=max(k_i)-min(k_i), such that a large R value means a greater importance of the factor.

For example, consider Table 3, where K_1 to K_3 values refer to the sum of the liquefaction ratio of all levels in factor A, factor B, and factor C. Meanwhile, k_1 to k_3 values represent the average values corresponding to K_1 to K_3 values. The calculation processes for K_1=164.9, k_1=55.0, and R=15.0 are shown below:

$$K_1=55.4+53.8+55.7=164.9;\ k_1=K_1/3=55.0;\ R=66.8-51.8=15.0 \quad (2)$$

And so on, for K_2, K_3, k_2 and k_3 calculations.

Fourier transform infrared spectroscopy (FTIR)

Fourier transform infrared (FT-IR) absorption spectra ranged from 4000 to 600 cm^{-1}. The spectra were recorded by Perkin Elmer Spectrum 65, and the resolution was 1 cm^{-1}.

RESULTS AND DISCUSSION

Compositional Analysis of *Salix psammophila*

The composition analysis of *S. psammophila* was performed by Changsha Willsun Technology Co., Ltd., China. The air-dried carbon and hydrogen were determined using an automatic carbon hydrogen analyzer (WS-CH100). The air-dried moisture, ash, and volatile matter were determined with an automatic industrial analyzer (WS-G808), and the air-dried higher heating value (HHV) was determined with an automatic calorimeter (WS-C502).

As shown in Table 1, the carbon and hydrogen contents of *S. psammophila* were 13.3% and 4.98%, respectively. *Salix psammophila* had a low content of moisture (3.07%) and ash (0.87%), but a high content of volatiles (82.8%). The HHV was 4684 $cal \cdot g^{-1}$, which was 33.1% lower than that of standard coal (7000 $cal \cdot g^{-1}$). The main components of *S. psammophila* were cellulose, hemicellulose, and lignin contents, which had been analyzed and verified by many researchers (Li *et al*. 2013).

Table 1. Proximate Analysis and Compositions of *Salix psammophila* [a]

C (%)	H (%)	Moisture (%)
13.3	4.98	3.07
Ash (%)	Volatile matter (%)	HHV ($cal \cdot g^{-1}$)
0.87	82.8	4684

[a] All measured on air-dried basis

Orthogonal Experiment Design and Results

The main factors affecting the hydrothermal liquefaction of *S. psammophila* were reaction temperature, reaction time, and solid-liquid ratio (Li *et al.* 2013).

In all chemical transformations involving the interaction of two or more species, initiation of the reaction is triggered by collision events of the reacting species. The frequency and strength of such collisions are certainly very dependent on the temperature of the reaction, since molecular motion is strongly dependent on temperature (Masa *et al.* 2019). Arrhenius formulated an equation relating the dependence of the rate constant (k) of a chemical reaction on the reaction temperature (T), $k = Ae^{-E_a / RT}$ (Masa *et al.* 2019), which is widely applied for studying chemical kinetics. The pre-exponential factor or frequency factor A is a measure of the rate at which collisions occur, E_a is the activation energy, the minimum kinetic energy that the reactants must have in order to form a product(s), while R is the universal gas constant. If we consider the conversion of reactants *S. psammophila* into the products, the molecules of *S. psammophila* must come into contact with each other, resulting in breakage, distortion, or re-arrangement of bonds and atoms. Thereby, extensive depolymerization occurs in *S. psammophila*. This increases both the

concentration of free radicals and probability of repolymerization of fragmented species. The competition among hydrolysis, fragmentation, and repolymerization reactions defines the role of temperature during pyrolysis. Depolymerization of biomass is a dominant reaction during initial stages of pyrolysis. Repolymerization and gaseous reactions become active at high temperatures, resulting in the formation of gases and the free radical reactions and thus leading to char formation (Akhtar and Amin 2011). Therefore, a suitable temperature usually yields higher amounts of liquefaction products. Moreover, the thermal decomposition temperature of IL ([Bmim]Cl) was approximately 257 °C. Thus, the temperature set in this study ranged from 180 to 240 °C.

Table 2. Levels and Factors Affecting the Hydrothermal Liquefaction of *S. psammophila*

Level	Factors		
	Temperature A (°C)	Reaction Time B (min)	Solid-liquid Ratio C (g/g)
1	180	30	1:0.5
2	200	90	1:1
3	240	150	1:1.5

Table 3. Orthogonal Experiment List, Liquefaction Ratio Results, and the Range Analysis Data

Experiment No.	Factors					
	Temperature A (°C)	Reaction Time B (min)	Solid-liquid Ratio C (g/g)	Mass of *S. psammophila* (g)	Mass of [Bmim]Cl (g)	Liquefaction Ratio (%)
1	180	30	1:0.5	0.5023	0.2546	55.4
2	180	90	1:1	0.5061	0.5080	53.8
3	180	150	1:1.5	0.5011	0.7593	55.7
4	200	30	1:1	0.5007	0.5031	48.4
5	200	90	1:1.5	0.5003	0.7561	57.6
6	200	150	1:0.5	0.5004	0.2523	49.4
7	240	30	1:1.5	0.5007	0.7589	49.9
8	240	90	1:0.5	0.4999	0.2504	75.6
9	240	150	1:1	0.5005	0.5085	74.9
K_1	164.9	153.7	180.4			
K_2	155.4	187.0	177.1			
K_3	200.4	180.0	163.2			
k_1	55.0	51.2	60.1			
k_2	51.8	62.3	59.0			
k_3	66.8	60.0	54.4			
R	15.0	11.1	5.7			

Optimization of the reaction time is necessary for effective destruction of organic compounds in *S. psammophila*. Many studies have reported that a shorter reaction time might usually be favored, but that a longer reaction time might suppress the liquid yields, which could be explained by the cracking of bio-oil or intermediate products to gases and the formation of chars by condensation, cyclization, and repolymerization (Jindal and Jha 2016). The optimal reaction time here was determined by the condition with the maximum liquefaction ratio. Reaction time was set at 30, 60, and 150 min in this study.

To determine the optimal reaction parameters for the highest liquefaction yield of *S. psammophila,* an $L_9(3^4)$ was employed to assign the considered factors as shown in Table 2, which was an orthogonal array with three factors and three levels. The following three factors were analyzed: temperature (factor A), reaction time (factor B), and solid-liquid ratio (factor C). Nine experiments were carried out to achieve the optimization process according to Table 3. Based on Table 3, the range of the liquefaction ratio ranged from 48.4% to 75.6%. As mentioned, a higher average value for k_i demonstrates that the corresponding level has a bigger effect on liquefaction ratio. Therefore, the best levels for the three factors were as follows: temperature was 240 °C, reaction time was 90 min, and solid-liquid ratio was 1:0.5. Meanwhile, the *R* value demonstrates the significance of the factor's influence and a larger *R* means that the factor has a bigger impact on the liquefaction ratio (Gao *et al.* 2015; Shen *et al.* 2016). In Table 3, the decreasing order $R_A > R_B > R_C$ indicates that the difference in temperature influenced the liquefaction ratio the most, followed by the reaction time and solid-liquid ratio. Moreover, the appropriate solid-liquid ratio could not only facilitate liquefaction reaction, but it also reduced the occurrence of repolymerization during later stage. In Table 3, it could be observed that different solid-liquid ratios (1:0.5; 1:1; 1:1.5) seemed to have less influence on the *S. psammophila* liquefaction in this study.

Recyclability of the Ionic Liquid [Bmim]Cl

Ionic liquids are effective solvents/media for biomass utilization. The unique properties of IL enable them to effectively dissolve and/or convert the biomass into various types of products (Yoo *et al.* 2017). Generally, the prices of ILs are much higher than commercial solvents. Therefore, the efficiency with which ILs are recycled and reused is very important. To make this *S. psammophila* liquefaction process sustainable and cost-friendly, two cycles recycling-reusability of the IL [Bmim]Cl were carried out. The water phase with [Bmim]Cl derived from the first liquefaction reaction was evaporated in a rotary evaporator, the obtained [Bmim]Cl was reused for orthogonal experiment, and the liquefaction ratio results were presented in Table 4. Similarly, [Bmim]Cl recycled from the second liquefaction reaction was reused for another orthogonal experiment, and the liquefaction ratio results were demonstrated in Table 5. Compared with the *S. psammophila* liquefaction ratio in Table 3, Table 4, and Table 5, it was observed that the liquefaction ratios displayed minimal difference under the same reaction condition. Moreover, it should be noted that under the optimized liquefaction conditions (temperature was 240 °C, the reaction time was 90 min, and solid-liquid ratio was 1:0.5), the corresponding liquefaction ratios (75.6%, 74.8%, and 73.8%) remained the highest, with nearly identical values. Consequently, the fresh, the first reused and the second reused [Bmim]Cl exhibited high stability.

Fourier transform infrared (FT-IR) absorption spectra were measured. Among the orthogonal experiments listed in Tables 3 to 5, a random FT-IR spectrum of the freshly used, firstly reused, and secondarily reused IL [Bmim]Cl were measured and shown in Fig. 2. The peak at 2112 cm^{-1} is attributed to C=N stretching vibration in imidazole ring. The peak at 1644 cm^{-1} corresponds to imidazole ring skeleton vibration. The peak at 1174 cm^{-1} is assigned to alkyl carbon C-N stretching vibration. The peak at 647 cm^{-1} is ascribed to C-Cl stretching vibration. The FT-IR spectra confirmed that there were no significant peak changes after the first and the second reuse compared with that of the fresh used [Bmim]Cl, further indicating the high stability IL [Bmim]Cl.

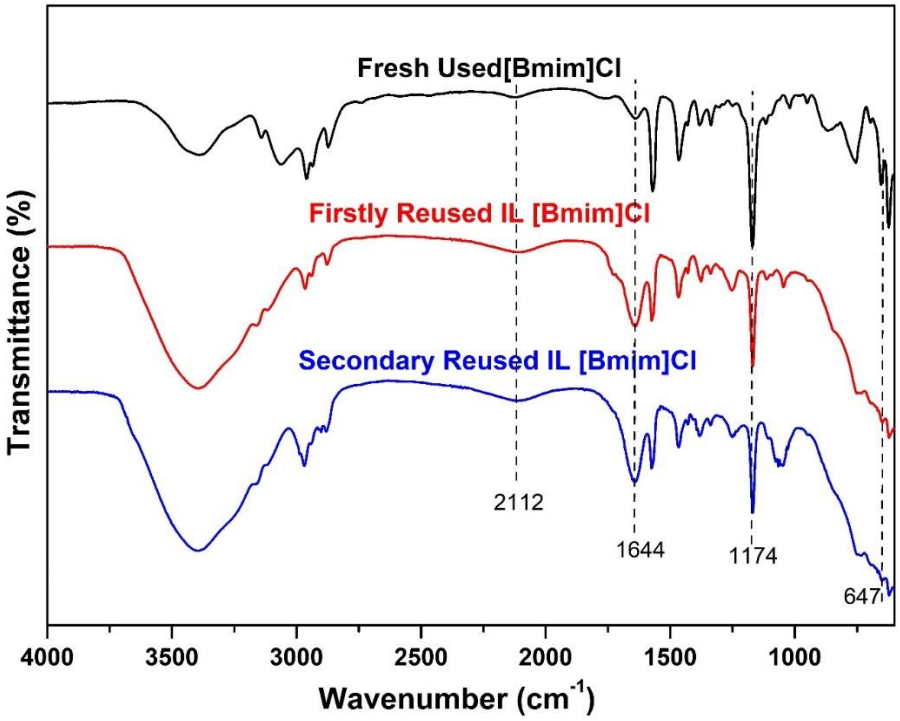

Fig. 2 FT-IR spectra of the fresh used, the firstly reused and the secondary reused IL [Bmim]Cl

Table 4. The First Reuse of [Bmim]Cl for Orthogonal Experiment and the Liquefaction Ratio Results

Experiment No.	Factors					
	Temperature A (°C)	Reaction Time B (min)	Solid-liquid Ratio C (g/g)	Mass of *S. psammophila* (g)	Mass of [Bmim]Cl (g)	Liquefaction Ratio (%)
1	180	30	1：0.5	0.5013	0.2546	42.3
2	180	90	1:1	0.5008	0.5080	45.1
3	180	150	1:1.5	0.5006	0.7593	51.8
4	200	30	1:1	0.5031	0.5031	47.7
5	200	90	1:1.5	0.5013	0.7561	55.1
6	200	150	1:0.5	0.5011	0.2523	45.0
7	240	30	1:1.5	0.5061	0.7589	68.1
8	240	90	1:0.5	0.4998	0.2504	74.8
9	240	150	1:1	0.5036	0.5085	65.6

Table 5. The Second Reuse of [Bmim]Cl for Orthogonal Experiment and Liquefaction Ratio Results

Experiment No.	Factors					
	Temperature A (°C)	Reaction Time B (min)	Solid-liquid Ratio C (g/g)	Mass of *S. psammophila* (g)	Mass of [Bmim]Cl (g)	Liquefaction Ratio (%)
1	180	30	1:0.5	0.5017	0.2546	51.1
2	180	90	1:1	0.5016	0.5080	49.4
3	180	150	1:1.5	0.5007	0.7593	60.1
4	200	30	1:1	0.5005	0.5031	53.9
5	200	90	1:1.5	0.5022	0.7561	47.8
6	200	150	1:0.5	0.5015	0.2523	45.1
7	240	30	1:1.5	0.5017	0.7589	65.0
8	240	90	1:0.5	0.5006	0.2504	73.8
9	240	150	1:1	0.5012	0.5085	63.4

GC Analysis Results of Oil Phase Products

The chemical components in the oil phase were examined through GC analysis.

Table 6. GC Results of the Liquefied Products Based on Different States of [Bmim]Cl at the Optimal Liquefaction Conditions

Compound Name	RT[a] (min)	Concentration (mg/L)		
		Fresh Used IL [Bmim]Cl [b]	Firstly Reused IL [Bmim]Cl [c]	Twice Reused IL [Bmim]Cl [d]
Ethane, propane	2.628	0.77209	0.71317	0.72913
1-Octane	4.173	113.68	101.17	94.257
Acetone	4.576	20.103	5.5977	6.8642
Methyl acetate	4.755	37.954	38.373	41.722
Ethyl acetate	6.085	9.3906	9.1350	9.3267
Methanol	6.478	20.269	19.074	19.328
Ethanol	7.351	1009.2	1006.3	16.657
Ethyl propionate	8.207	452.23	414.00	391.52
Methyl butyrate	8.971	9.9544	13.330	9.1603
2-Butanol	10.031	0.67488	0.68054	---[e]
Propanol	10.418	1.2295	1.3094	1.4379
2-Methyl-1-propanol	11.316	3.8518	3.47682	2.3809
2-Pentanol	12.132	26.760	23.365	21.006
1-Butanol	12.253	31.900	27.415	24.861
Furfural	12.354	90.539	78.718	70.533
Isopentyl alcohol	12.989	62.408	54.890	48.696
1-Pentanol	13.567	0.53080	0.37269	0.41214
Isohexanol	14.154	1.5476	1.6466	1.7577
1-Hexanol	14.822	0.49044	0.58366	0.80848
Isoheptyl alcohol	15.424	0.86410	1.2425	0.76474
15 Hydrocarbon	15.791	173.23	198.94	151.60
1-Heptanol	16.207	10.916	10.566	13.006
16 Hydrocarbon	16.941	22.127	21.573	19.887

[a] Retention time; [b] The compounds obtained by GC based on the fresh used [Bmim]Cl in experiment No. 8 experiment; [c] The compounds obtained by GC based on the firstly reused [Bmim]Cl in experiment No.8 experiment; [d] The compounds obtained by GC based on the secondary reused [Bmim]Cl in experiment No. 8 experiment; and [e] undetectable

As a representative, the compounds identified by GC at the optimal liquefaction conditions (temperature - 240 °C, reaction time - 90 min, and solid-liquid ratio - 1:0.5) are listed in Table 6. Table 6 indicated that the compounds obtained could be classified into several groups, including alcohols, esters, aldehydes, ketones, long-chain alkanes, and furfurals. It was noticed that the compounds acquired based on the nature of IL, such as fresh IL, the firstly reused IL, and secondary reused IL [in experiment No.8 experiment (at the optimal hydrothermal liquefaction conditions) were of the same types and their concentration ($mg \cdot L^{-1}$) displayed little differences. It could be suggested that the optimal liquefaction conditions determined by the orthogonal experiments were reliable. To some extent, it was confirmed that the recycling and reusing of [Bmim]Cl displayed high stability with nearly identical liquefaction products and concentration. Moreover, it was found that the dominant liquefied compounds were ethanol, ethyl propionate, 15 hydrocarbon, 1-octane, furfural, and isopentyl alcohol.

Brief Explanation on *Salix psammophila* Decomposition Mechanism in Hydrothermal Liquefaction

Hydrothermal liquefaction is a thermo-chemical conversion process that uses water as a reaction medium at elevated pressure and temperature (Kumar 2022). Generally, the pathway of hydrothermal liquefaction comprises three major steps, depolymerization, followed by decomposition, and recombination (Gollakota *et al.* 2018).

Depolymerization of *S. psammophila* involves a sequential dissolving of macromolecules. Adequate dissolution was achieved by the utilization of [Bmim]Cl. Known as one of the optimal solvents for lignocellulosic material, the IL [Bmim]Cl was selected here. The dissolution mechanism of cellulose component of *S. psammophila* in the presence of [Bmim]Cl could be attributed to the nature of the imidazolium cation and the relatively strong electronegativity and small size of the chloride ion (Dadi *et al.* 2006). The imidazolium cation with its electron-rich aromatic π system interacts with cellulose hydroxyl oxygen atoms *via* non-bonding or π electrons and in addition prevents crosslinking of the cellulose molecules. The chloride ion attacks the free hydroxyl groups and deprotonates cellulose. The activity of [Bmim]Cl was effective in breaking down the H-bond network of cellulose (Zhang *et al.* 2017). Moreover, in depolymerization process, the decisive parameters temperature and pressure in this work changed the structure of the long chain polymers to shorter chain products.

Decomposition of the *S. psammophila* monomers was accomplished by cleavage, dehydration (the loss of water molecule), and decarboxylation (loss of CO_2 molecule) steps (Gollakota *et al.* 2018). *Salix psammophila* was hydrolyzed to form polar oligomers and monomers. Water is present in all biomass, including *S. psammophila*. Hydrothermal liquefaction could handle and liquefy biomass with any level of moisture contents. Here the addition of water served as both solvent and reactant in the hydrothermal liquefaction. Under the condition of hydrothermal liquefaction, the structure and properties of water changed dramatically (Kruse and Dinjus 2007) when its temperature was raised, resulting in the rapid drop of dielectric constant. Consequently, the ion product decreased and hydrogen bonding became weak. Additionally, water behaved like a nonpolar component, resulting in an increase in solubility of organic molecules. Deconstruction of cellulose and hemicellulose carbohydrate polymers by water into their constituent C5 and C6 sugars occurred, leading to subsequent catalytic reforming into other chemical intermediates and products by different types of reactions (Zhang *et al.* 2016). Decomposition and deoxygenation were the major reactions, which produced degradation products containing

acids, aldehydes, and aromatic compounds (Akhtar and Amin 2011; Gollakota *et al*. 2018). In addition, the hydrolyzed and depolymerized products usually undergo secondary reactions. Major reactions among these were condensation, dehydrations, and isomerization. Alcohols and aldehydes were produced by the results of the secondary reactions (Xu and Lancaster 2008; Zou *et al.* 2011), while furfurals were formed as secondary intermediates.

Under certain conditions, the unavailability of the hydrogen or the concentration of the free radicals were excessively large, such that the fragments were recombined or repolymerized. Recombination and repolymerization process usually generate acids, alcohols, aldehydes, esters, ketones, and other aromatic compounds (Chornet and Overend 1985). The liquefied products detected and listed in Table 6 were in accordance with the above brief mechanism.

CONCLUSIONS

1. The optimal reaction parameters (temperature was 240 °C, reaction time was 90 min, and solid-liquid ratio was 1:0.5) were determined by orthogonal experiments. Under the optimized liquefaction condition, the liquefaction ratio of *Salix psammophila* reached 75.6%.
2. The FT-IR spectra confirmed that there were no significant peak changes after the first and the second reuse compared with that of the freshly used [Bmim]Cl, indicating the stability of IL [Bmim]Cl.
3. The IL [Bmim]Cl used for three consecutive liquefaction reactions displayed high liquefaction ratios (75.6%, 74.8%, and 73.8%). GC results of the liquefied products exhibited nearly identical liquefaction products and concentration.
4. The liquefied products obtained by GC confirmed the presence of value-added chemicals, such as acids, alcohols, aldehydes, esters, ketones, and furfural.

The hydrothermal liquefaction is one of the promising technologies to produce highly valuable chemicals from *S. psammophila*. The desired compounds C7 to C8 that are desirable for transportation fuels were not found due to the limited operating conditions. In the near future, there is a need for scale-up experiments and further studies about *S. psammophila* liquefaction mechanism are required.

ACKNOWLEDGEMENTS

This work was financially supported by the Interdisciplinary Research Fund of Inner Mongolia Agricultural University (BR22-15-02), the Central Government Guides Local Science and Technology Development Fund Projects (2022ZY0066), the Innovative Entrepreneurship Training Program of Inner Mongolia (202310129016, 202210129017, 202210129028)

REFERENCES CITED

Akhtar, J., and Amin, N. A. S. (2011). "A review on process conditions for optimum bio-oil yield in hydrothermal liquefaction of biomass," *Renewable and Sustainable Energy Reviews* 15(3), 1615-1624. DOI: 10.1016/j.rser.2010.11.054

Chornet, E., and Overend, R. (1985). "Biomass liquefaction: An overview," in: *Proceedings of the International Conference on Fundamentals of Thermochemical Biomass Conversion*, Elsevier Applied Science, New York, NY, USA, pp. 967-1002.

Dadi, A. P., Varanasi, S., and Schall, C. A. (2006). "Enhancement of cellulose saccharification kinetics using an ionic liquid pretreatment step," *Biotechnology and Bioengineering* 95(5), 904-910. DOI: 10.1002/bit.21047

Durak, H. (2019). "Hydrothermal liquefaction of *Glycyrrhiza glabra* L. (liquorice): Effects of catalyst on variety compounds and chromatographic characterization," *Energy Sources, Part A: Recovery, Utilization, and Environmental Effects* 42(20), 2471-2484. DOI: 10.1080/15567036.2019.1607947

Durak, H., and Genelb, S. (2023). "Characterization of bio-oil and bio-char obtained from black cumin seed by hydrothermal liquefaction: investigation of potential as an energy source," *Energy Sources, Part A: Recovery, Utilization, and Environmental Effects* 45(2), 3205-3215. DOI: 10.1080/15567036.2020.1714821

Gao, Y., Yu, B., Wang, X., Yuan, Q., Yang, H., Chen, H., and Zhang, S. (2015). "Orthogonal test design to optimize products and to characterize heavy oil *via* biomass hydrothermal treatment," *Energy* 88, 139-148. DOI: 10.1016/j.energy.2015.04.014

Gollakota, A. R. K., Kishore, N., and Gu, S. (2018). "A review on hydrothermal liquefaction of biomass," *Renewable and Sustainable Energy Reviews* 81, 1378-1392. DOI: 10.1016/j.rser.2017.05.178

Jindal, M., and Jha, M. (2016). "Hydrothermal liquefaction of wood: A critical review," *Reviews in Chemical Engineering* 32(4), 459-488. DOI: 10.1515/revce-2015-0055

Ji, Y., Lin, Q., Huang, Y., Rao, F., and Yu, W. (2019). "High-performance wood composites from desert shrub *Salix psammophila*," *Green Materials* 7(4), 177-184. DOI: 10.1680/jgrma.18.00093

Kruse, A., and Dinjus, E. (2007). "Hot compressed water as reaction medium and reactant," *The Journal of Supercritical Fluids* 39(3), 362-380. DOI: 10.1016/j.supflu.2006.03.016

Kubo, S., Hashida, K., Makino, R., Magara, K., Kenzo, T., Kato, A., and Aorigele (2013). "Chemical composition of desert willow (*Salix psammophila*) grown in the Kubuqi desert, Inner Mongolia, China: Bark extracts associated with environmental adaptability," *J. Ag. Food Chem.* 61(50), 12226-12231. DOI: 10.1021/jf4038634

Kumar, R. (2022). "A review on the modelling of hydrothermal liquefaction of biomass and waste feedstocks," *Energy Nexus* 5, article ID 100042. DOI: 10.1016/j.nexus.2022.100042

Li, C., Yang, X., Zhang, Z., Zhou, D., Zhang, L., Zhang, S., and Chen, J. (2013). "Hydrothermal liquefaction of desert shrub *Salix psammophila* to high value-added chemicals and hydrochar with recycled processing water," *BioResources* 8(2), 2981-2997. DOI: 10.15376/biores.8.2.2981-2997

Maldas, D., and Shiraishi, N. (1997). "Liquefaction of biomass in the presence of phenol and H_2O using alkalies and salts as the catalyst," *Biomass and Bioenergy* 12(4), 273-279. DOI: 10.1016/s0961-9534(96)00074-8

Masa, J., Barwe, S., Andronescu, C., and Schuhmann, W. (2019). "On the theory of electrolytic dissociation, the greenhouse effect, and activation energy in (electro) catalysis: A tribute to svante Augustus Arrhenius," *Chem. Eur. J*. 25(1) 158-166. DOI: 10.1002/chem.201805264.

Reina, L., Botto, E., Mantero, C., Moyna, P., and Menéndez, P. (2016). "Production of second generation ethanol using *Eucalyptus dunnii* bark residues and ionic liquid pretreatment," *Biomass and Bioenergy* 93, 116-121. DOI: 10.1016/j.biombioe.2016.06.023

Schenzel, A., Hufendiek, A., Barner-Kowollik, C., and Meier, M. A. R. (2014). "Catalytic transesterification of cellulose in ionic liquids: Sustainable access to cellulose esters," *Green Chemistry* 16(6), 3266-3271. DOI: 10.1039/C4GC00312H

Shen, Q., Zheng, Y., Li, S., Ding, H., Xu, Y., Zheng, C., and Thern, M. (2016). "Optimize process parameters of microwave-assisted EDTA method using orthogonal experiment for novel $BaCo_{3-\delta}$ perovskite," *Journal of Alloys and Compounds* 658, 125-131. DOI: 10.1016/j.jallcom.2015.10.194

Swatloski, R. P., Spear, S. K., Holbrey, J. D., and Rogers, R. D. (2002). "Dissolution of cellulose with ionic liquids," *Journal of the American Chemical Society* 124(18), 4974-4975. DOI: 10.1021/ja025790m

Vitz, J., Erdmenger, T., Haensch, C., and Schubert, U. S. (2009). "Extended dissolution studies of cellulose in imidazolium based ionic liquids," *Green Chemistry* 11(3), 417-424. DOI: 10.1039/B818061J

Xu, C., and Lancaster, J. (2008). "Conversion of secondary pulp/paper sludge powder to liquid oil products for energy recovery by direct liquefaction in hot-compressed water," *Water Research* 42(6-7), 1571-1582. DOI: 10.1016/j.watres.2007.11.007

Yoo, C. G., Pu, Y., and Ragauskas, A. J. (2017). "Ionic liquids: Promising green solvents for lignocellulosic biomass utilization." *Current Opinion in Green and Sustainable Chemistry* 5, 5-11. DOI: 10.1016/s0961-9534(96)00074-8

Zhang, Q., Hu, J., and Lee, D.-J. (2017). "Pretreatment of biomass using ionic liquids: Research updates," *Renewable Energy* 111, 77-84. DOI:10.1016/j.renene.2017.03.093

Zhang, X., Wilson, K., and Lee, A. F. (2016). "Heterogeneously catalyzed hydrothermal processing of C5–C6 sugars," *Chemical Reviews* 116(19), 12328-12368. DOI: 10.1021/acs.chemrev.6b00311

Zhong, Y., Gao, X., Zhang, W., Wang, X., and Wang, K. (2022). "Carboxylated nanocrystalline cellulose from *Salix psammophila* prepared by sulfuric acid hydrolysis combined with 2, 2, 6, 6-tetramethylpiperidine-1-oxyl (TEMPO)-oxidation," *BioResources* 17(1), 1373-1384. DOI: 10.15376/biores.17.1.1373-1384

Zhong, Y., Wang, K. B., Liu, Y. L., and Wang, X. (2020). "Preparation and characterization of *Salix psammophila* cellulose and mic-cellulose under the pretreatment of two kinds of acid," *Journal of Physics: Conference Series* 1605(1), article ID 012165. DOI: 10.1088/1742-6596/1605/1/012165

Zou, X., Qin, T., Wang, Y., and Huang, L. (2011). "Mechanisms and product specialties of the alcoholysis processes of poplar components," *Energy & Fuels* 25(8), 3786–3792. DOI: 10.1021/ef200726w

Article submitted: March 3, 2023; Peer review completed: June 24, 2023; Revised version received and accepted: July 16, 2023; Published: September 7, 2023.
DOI: 10.15376/biores.18.4.7341-7352